BL28B2
White Beam X-ray Diffraction

1. Introduction

BL28B2 is dedicated to multiple techniques using white X-rays in several research fields. It is a bending magnet beamline that provides white X-rays from a bending magnet source without passing through any optical devices. The techniques include (1) X-ray diffraction, (2) dispersive-type time-resolved X-ray absorption fine structures (DXAFS), and (3) X-ray imaging. The beamline supports various experiments such as the evaluation of structure materials using white X-ray diffraction imaging, the observation of dynamic structural changes during chemical reaction processes in catalysis and fuel-cell batteries using DXAFS, and the three-dimensional observation of metallic objects and fossils using high-energy X-ray microtomography. To improve and upgrade the measurement techniques using this beamline, the research and development of experimental techniques and instruments was conducted in FY2021.

2. Upgrades of measurement techniques

2-1. X-ray diffraction

To enhance the usability of the beamline as a general-purpose white X-ray beamline, we removed the conventionally used large table (Fig. 1(a)) and changed the layout of the beamline so that users can bring their own large equipment. With this change, we designed and introduced a stand for installing optical devices on the upstream side of the diffractometer. Figure 1(b) is a drawing of the new stand. The pillar of the stand was spaced from the diffractometer so as not to interfere with its operation. On the other hand, the upper part of the stand was designed to protrude toward the sample so that the slit could be installed near the sample. The height of the stand is the same as that of the previous table, so that the previous equipment can be used as it is. In addition, the stand is transportable so that the space on the upstream side of the diffractometer can be widened depending on the contents of the experiment. Figure 1(c) shows a photograph of this new stand when it was used in the experiment. Experiments can be performed in the same way as before, and it has become possible to handle even larger equipment brought in by users.

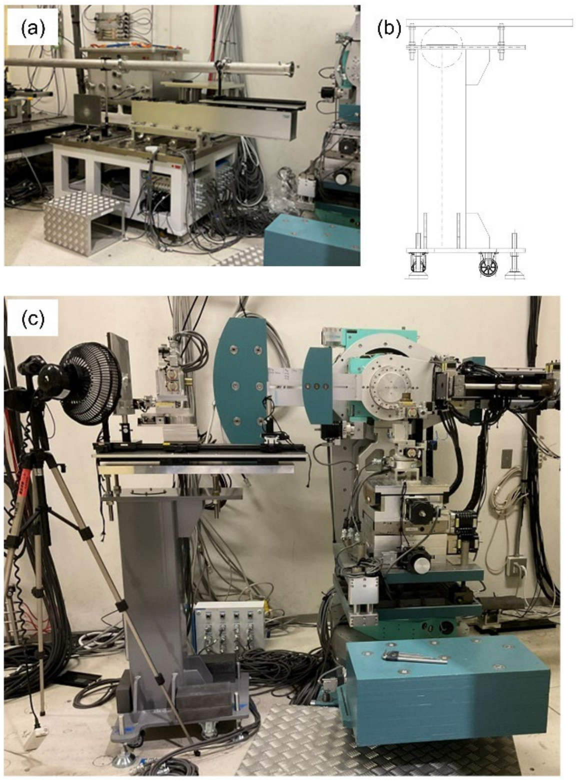

Fig. 1. Photograph of removed table (a), drawing of newly designed stand (b), and photograph of new stand (c).

2-2. High-energy X-ray microtomography

High-energy X-ray microtomography using white X-rays has a great potential to observe metallic objects and large dense materials such as fossils. A simple heavy metal filter composed of a tungsten plate of 0.5 mm thickness and a lead plate of 2 mm thickness for incident white X-rays makes it possible to use high-energy white X-rays with the peak energy of around 200 keV [1]. The high-energy X-ray beam has abundant photon flux. Therefore, it is expected to be applied to high-resolution observation even at the 200 keV region. By combining the high-resolution observation with a wide-field-of-view observation reported in the FY2019 annual report [2], a multiscale observation for a large dense object would be expected, which includes both the entire observation of the object and a localized high-resolution observation. As an upgrade of high-energy X-ray microtomography at the 200 keV region, a multiscale X-ray microtomography system was developed.

In the high-energy multiscale X-ray microtomography system, two types of X-ray imaging detector are employed. One is for the wide-field-of-view observation, and the other is for the high-resolution observation of the local structure. In the case of the former, an X-ray imaging detector capable of taking a projection image with the maximum field of view of 50 mm width was used. Both detectors are the so-called visible-light conversion-type indirect X-ray imaging detectors. A tandem-lens system was employed as the visible-light optics. As a scintillating material to convert incident X-rays into visible light, a $Lu_3Al_5O_{12}:Ce^+$ (LuAG) ceramics plate of 500 μm thickness was used. In the case of the high-resolution X-ray detector, a thick scintillator made the X-ray image blurry because the high-energy X-rays at the 200 keV region easily penetrated the scintillator, resulting in the increase in the intensity of the undesired signals from the penetration path, which was longer than the effective depth of focus of the lens system. To address this issue, the aperture of the lens system was decreased to increase the effective depth of focus on the scintillator. In the actual setup of high-energy multiscale X-ray microtomography, the effective pixel size and the field of view of the wide-field-of-view detector were 12.02 μm and 49.2 mm, respectively. In comparison, those of the high-resolution detector were 1.61 μm and 7.4 mm, respectively. A photograph of the detector system installed at optics hutch 3 is shown in Fig. 2. The propagation distances from the sample set at optics hutch 2 to each detector were 1.5 m for the high-resolution detector and 3.5 m for the wide-field-of-view detector. The high-resolution detector could be removed by a horizontal translation stage when observing the sample with the wide-field-of-view detector. This meant that the high-resolution and wide-field-of-view modes could be easily switched while the sample remains on the same stage.

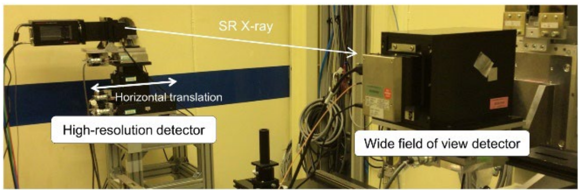

Fig. 2. Photograph of detector system for multiscale high-energy X-ray microtomography.

As a demonstration of high-energy multiscale X-ray microtomography, a limestone sample was observed [3]. Sectional images of the limestone sample observed with the wide-field-of-view and high-resolution detectors are shown in Figs. 3(a) and 3(b), respectively. In the high-resolution observation, the circular part shown in Fig. 3(a) was observed. A magnified image of the square region in Fig. 3(b) is shown in the left panel of Fig. 3(c). For comparison, the same region in the wide-field-of-view observation is also displayed in the right panel. The detailed structure of the fossil inclusion was clearly observed in the high-resolution image.

As a future work, the measurement condition towards a higher spatial resolution will be evaluated using an optimized thinner scintillator.

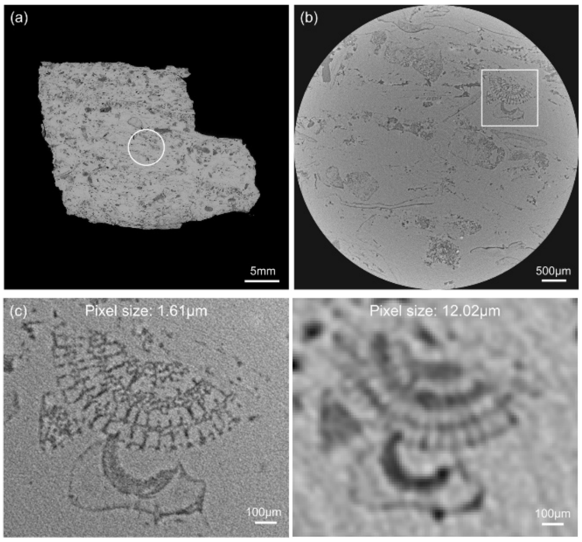

Fig. 3. Sectional images of limestone sample observed with (a) wide-field-of-view and (b) high-resolution detectors. (c) Left: magnified image of the square shown in (b). Right: the same region in the wide-field-of-view observation.

3. Removal of beamline equipment

As part of the plan to enhance time-resolved experiments in the XAFS beamline restructuring project, it was decided to end time-resolved XAFS experiments using the DXAFS system at BL28B2 in FY2021 and to conduct them using the QXAFS measurement system at BL36XU thereafter.

On the basis of this reorganization plan, after user experiments using DXAFS were conducted in November 2021, the DXAFS measurement system was removed from optics hutch 2 in December 2021.

4. Conclusion

Upgrades of the beamline and measurement techniques in FY2021 are presented. In addition to these upgrades, a project to introduce an automated X-ray microtomography system is under way. The system will be operational in FY2022.

Hoshino Masato, Kajiwara Kentaro, Kato Kazuo, and Yasutake Masahiro

Japan Synchrotron Radiation Research Institute

References:

[1] Hoshino, M., Uesugi, K. Shikaku, R. & Yagi, N. (2017). *AIP Adv.* **7**, 105122.

[2] Hoshino, M., Umetani, K., Kato, K. & Kajiwara, K. (2020). *SPring-8/SACLA Annual Report FY2019,* 55–58.

[3] Hoshino, M., Uesugi, K. & Yagi, N. (2021). *Kinzoku.* **91**, 198–207.